Int. J. Solids Structures, 1977, Vol. 13, pp. 957–970. Pergamon Press. Printed in Great Britain

BUCKLING OF ELASTIC–PLASTIC CYLINDRICAL PANEL UNDER AXIAL COMPRESSION

VIGGO TVERGAARD
Department of Solid Mechanics, The Technical University of Denmark, Lyngby, Denmark

(*Received* 25 *January* 1977)

Abstract—The buckling behaviour is investigated for an axially compressed elastic–plastic cylindrical panel of the type occurring in stiffened shells. The bifurcation stress is determined analytically and an asymptotically exact expansion is obtained for the initial post-bifurcation behaviour in the plastic range. For panels with small initial imperfections the behaviour is analysed asymptotically on the basis of the hypoelastic theory that results from neglecting the effect of elastic unloading. The imperfection-sensitivity of an elastic–plastic panel is also computed numerically by a linear incremental method, and the results are compared with the results of the asymptotic analysis. For a low hardening material the panel is found to be imperfection-sensitive in the whole range of curvatures considered, whereas for a high hardening material the panel is only imperfection-sensitive if the curvature exceeds a certain value.

1. INTRODUCTION

The type of axially compressed cylindrical panels to be considered here occur between stiffeners in longitudinally stiffened cylindrical shells. When the stiffeners on such cylindrical shells are sufficiently close, the critical bifurcation mode is an overall mode with a circumferential wavelength much longer than the stiffener spacing. However, for larger spacing of the stiffeners, local buckling between stiffeners may be the critical mode. In the present paper the interest shall centre on this local buckling of the cylindrical panels between the stiffeners.

The initial post-buckling behaviour of elastic cylindrical panels has been investigated by Koiter [1], on the basis of the general theory of elastic stability [2]. This investigation shows that the post-buckling behaviour is stable for sufficiently flat panels in agreement with the behaviour of plates, while more curved panels have unstable post-buckling behaviour. The initial post-buckling analysis has been extended by Stephens [3] to also account for the torsional rigidity of the stiffeners and for the effect of internal pressure, which tend to increase the bifurcation stress and to decrease the imperfection-sensitivity. Post-buckling analyses have also been carried out for orthotropic elastic panels with shear deformability [4] and for sandwich panels [5].

The present paper gives an investigation of the post-buckling behaviour and the imperfection-sensitivity of elastic–plastic cylindrical panels compressed into the plastic range. The bifurcation behaviour at the tangent modulus load is determined analytically, and in cases where the bifurcation mode is unique Hutchinson's asymptotic theory [6, 7] is employed to obtain expressions for the initial post-bifurcation behaviour. For the effect of small initial imperfections an asymptotic analysis is carried out, based on neglecting the influence of elastic unloading. This type of hypoelastic asymptotic analysis was developed by Hutchinson and Budiansky [8] for the case of a cruciform column and has also been used by Needleman and Tvergaard [9] for an axially compressed square plate. The behaviour of imperfect cylindrical panels is also computed numerically by a linear incremental method, and the results are compared with the asymptotic results.

2. PROBLEM FORMULATION

The narrow cylindrical panel is taken to be part of a longitudinally stiffened circular cylindrical shell under axial compression. Here the cylindrical panel occurs as a section of the shell bounded by two neighbouring stiffeners, and the local buckling mode of interest is one in which the stiffeners remain straight, while the shell buckles in a short wave pattern between the stiffeners.

The shell has the thickness h, the radius R, and the circumferential distance b between the equally spaced stiffeners (Fig. 1). The main effect of the stiffeners is to prevent waviness of

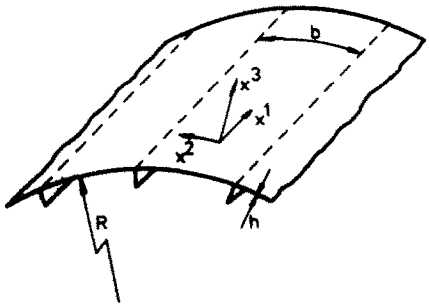

Fig. 1. Part of axially stiffened circular cylindrical shell.

radial deflections along their lines of attachment. As in Koiter's analysis of the elastic cylindrical panel[1], this is the only stiffener constraint we shall account for in the present investigation. Thus, we shall assume that there is no constraint on tangential shell displacements along the stiffeners, and that the torsional rigidity of the stiffeners can be neglected. It may be added that an analysis taking account of all stiffener constraints would follow the line of that given in Ref. [10] for a flat stiffened panel.

In the following we let a point on the shell middle surface be identified by the coordinates $(x^1, x^2) = (x, s)$, where x and s are measures of distance in axial and in circumferential direction, respectively. The displacements of the shell middle surface are v^α in the direction of the surface base vectors and w in the direction of the outward surface normal. Then, within the context of Donnell–Mushtari–Vlasov shell theory the increment of the membrane strain tensor $\dot{e}_{\alpha\beta}$ and the increment of the bending strain tensor $\dot{\kappa}_{\alpha\beta}$ are

$$\dot{e}_{\alpha\beta} = \frac{1}{2}(\dot{v}_{\alpha,\beta} + \dot{v}_{\beta,\alpha}) - d_{\alpha\beta}\dot{w} + \frac{1}{2}(w_{,\alpha}\dot{w}_{,\beta} + \dot{w}_{,\alpha}w_{,\beta})$$
$$\dot{\kappa}_{\alpha\beta} = \dot{w}_{,\alpha\beta} \tag{2.1}$$

Here $(\,)_{,\alpha}$ denotes covariant differentiation, and $(\dot{})$ denotes differentiation with respect to some monotonically increasing parameter that characterizes the loading history. Furthermore, $a_{\alpha\beta}$ and $d_{\alpha\beta}$ are the covariant components of the metric tensor and the curvature tensor, respectively, for the undeformed middle surface.

The three dimensional stress increments $\dot{\sigma}^{ij}$ and strain increments $\dot{\eta}_{kl}$ in the shell material are assumed to be related by the equations

$$\dot{\sigma}^{ij} = L^{ijkl}\dot{\eta}_{kl} \tag{2.2}$$

with $L^{ijkl} = L^{jikl} = L^{klij}$. Here, Latin indices range from 1 to 3, while Greek indices range from 1 to 2. The instantaneous moduli L^{ijkl} have two branches, one corresponding to plastic loading, the other to elastic unloading.

The theory of plasticity employed here is small-strain J_2-flow theory with isotropic hardening. In the three dimensional x^i-coordinate system with metric tensor g_{ij} the instantaneous moduli are

$$L^{ijkl} = \frac{E}{1+\nu}\left\{\frac{1}{2}(g^{ik}g^{jl} + g^{il}g^{jk}) + \frac{\nu}{1-2\nu}g^{ij}g^{kl} - f\frac{s^{ij}s^{kl}}{\sigma_e^2}\right\} \tag{2.3}$$

where E and ν are Young's modulus and Poisson's ratio, respectively, and

$$s^{ij} = \sigma^{ij} - \frac{1}{3}g^{ij}g_{kl}\sigma^{kl}, \qquad \sigma_e = \left\{\frac{3}{2}g_{ik}g_{jl}s^{ij}s^{kl}\right\}^{1/2} \tag{2.4}$$

$$f(\sigma_e) = \begin{cases} \dfrac{3}{2}\dfrac{E/E_t - 1}{E/E_t - (1-2\nu)/3}, & \text{for } \sigma_e = (\sigma_e)_{\max} \text{ and } \dot{\sigma}_e > 0 \\ 0, & \text{for } \sigma_e < (\sigma_e)_{\max} \text{ or } \dot{\sigma}_e < 0. \end{cases} \tag{2.5}$$

Here the initial value of $(\sigma_e)_{max}$ is the yield stress σ_y, and the tangent modulus E_t is the slope of the uniaxial stress–strain curve. The representation of uniaxial stress–strain behaviour chosen is a piecewise power law with continuous tangent modulus

$$\epsilon = \begin{cases} \dfrac{\sigma}{E}, & \text{for } \sigma \le \sigma_y \\ \dfrac{\sigma_y}{E}\left[\dfrac{1}{n}\left(\dfrac{\sigma}{\sigma_y}\right)^n - \dfrac{1}{n} + 1\right], & \text{for } \sigma > \sigma_y \end{cases} \tag{2.6}$$

where n is the strain hardening exponent.

Since the stress state in the shell is approximately plane, only the in-plane stresses enter into the constitutive relations, and we can write

$$\dot{\sigma}^{\alpha\beta} = \hat{L}^{\alpha\beta\gamma\delta}\dot{\eta}_{\gamma\delta} \tag{2.7}$$

where the tensor of in-plane moduli is given by

$$\hat{L}^{\alpha\beta\gamma\delta} = L^{\alpha\beta\gamma\delta} - \frac{L^{\alpha\beta 33}L^{\gamma\delta 33}}{L^{3333}} \tag{2.8}$$

and the Lagrangian strain increment tensor at distance x^3 outward from the shell middle surface is approximated by

$$\dot{\eta}_{\alpha\beta} = \dot{\epsilon}_{\alpha\beta} - x^3\dot{\kappa}_{\alpha\beta}. \tag{2.9}$$

The membrane stress tensor $N^{\alpha\beta}$ and the moment tensor $M^{\alpha\beta}$ are taken to be

$$N^{\alpha\beta} = \int_{-h/2}^{h/2} \sigma^{\alpha\beta}\,dx^3, \qquad M^{\alpha\beta} = -\int_{-h/2}^{h/2} \sigma^{\alpha\beta}x^3\,dx^3. \tag{2.10}$$

Using eqns (2.7) and (2.9) in (2.10) gives incremental relations for $\dot{N}^{\alpha\beta}$ and $\dot{M}^{\alpha\beta}$ in terms of $\dot{\epsilon}_{\gamma\delta}$ and $\dot{\kappa}_{\gamma\delta}$. Now, within the context of Donnell–Mushtari–Vlasov shell theory the incremental principle of virtual work takes the form

$$\int_A [\dot{N}^{\alpha\beta}\delta\dot{\epsilon}_{\alpha\beta} + \dot{M}^{\alpha\beta}\delta\dot{\kappa}_{\alpha\beta} + N^{\alpha\beta}\dot{w}_{,\alpha}\delta\dot{w}_{,\beta}]\,dA = (EVW)^{\cdot} \tag{2.11}$$

where $(EVW)^{\cdot}$ is the increment of the external virtual work. In the following the integration area A shall be chosen according to the smallest repeatable intervals in the periodic deformation pattern.

As the buckling pattern is periodic in circumferential direction, due to the constant stiffener spacing, we need only consider a shell-section between the centres $x^2 = 0$, b of the two neighbouring cylindrical panels. Due to the symmetry of mode displacements about these panel centres the boundary conditions can be specified as

$$\frac{\partial v_1}{\partial x^2} = v_2 = \frac{\partial w}{\partial x^2} = \frac{\partial^3 w}{\partial (x^2)^3} = 0 \qquad \text{at } x^2 = 0, b. \tag{2.12}$$

Across the line of attachment of a stiffener we require continuity of all field quantities, except for the possible discontinuity of the transverse shear force resulting from the constraint

$$\frac{\partial w}{\partial x^1} = 0 \qquad \text{at } x^2 = b/2. \tag{2.13}$$

In axial direction the mode displacements are periodic, and the resultant axial load is specified

by the load parameter λ, as

$$\int_0^b N^{11}\,dx^2 = \lambda\sigma_I^{11}hb \tag{2.14}$$

where σ_I^{11} is a constant.

3. PLASTIC BIFURCATION AND POST-BIFURCATION BEHAVIOUR

The stress state in the perfect cylindrical shell prior to bifurcation consists of a constant uniaxial stress $\sigma^{11} = \lambda\sigma_I^{11}$ at every point of the shell. Thus, at any load level the components of the in-plane moduli $\hat{L}^{\alpha\beta\gamma\delta}$ are constant throughout the shell, and the lowest bifurcation load can be determined as that of an elastic orthotropic shell with moduli equal to the instantaneous plastic moduli. In the following we shall use the expressions E_1, E_2, E_{12} and E_G for the physical values of the plastic branches of $\hat{L}^{1111}$, $\hat{L}^{2222}$, $\hat{L}^{1122}$ and $\hat{L}^{1212}$, respectively, at the bifurcation point, and we shall use $D_1 = E_1h^3/12$, $D_2 = E_2h^3/12$, $D_{12} = E_{12}h^3/12$ and $D_G = E_Gh^3/6$.

For a complete unstiffened cylindrical shell, simply supported at the ends, the bifurcation modes are found of the form

$$\left.\begin{aligned} \overset{(1)}{v}_1 &= hc_1 \cos\frac{\pi x^2}{b}\cos\frac{\alpha\pi x^1}{b} \\ \overset{(1)}{v}_2 &= hc_2 \sin\frac{\pi x^2}{b}\sin\frac{\alpha\pi x^1}{b} \\ \overset{(1)}{w} &= h\cos\frac{\pi x^2}{b}\sin\frac{\alpha\pi x^1}{b} \end{aligned}\right\} \tag{3.1}$$

where $b = \pi R/m$ (m is the circumferential wave number); or in the form of an axisymmetric sinusoidal mode. The bifurcation stress σ_c corresponding to (3.1) is given by

$$\sigma_c = -\frac{[D_1\alpha^4 + 2(D_{12}+D_G)\alpha^2 + D_2]\left(\frac{\pi}{b}\right)^4 + E_2\frac{h}{R}\left(c_2\frac{\pi}{b}+\frac{1}{R}\right) - c_1E_{12}\frac{h}{R}\frac{\pi}{b}\alpha}{h\left(\frac{\alpha\pi}{b}\right)^2} \tag{3.2}$$

where

$$c_1 = \frac{E_G(E_{12}\alpha^2 - E_2)\frac{\alpha}{R}\frac{b}{\pi}}{(E_1\alpha^2+E_G)(E_2+E_G\alpha^2)-(E_{12}+E_G)^2\alpha^2} \tag{3.3}$$

$$c_2 = \frac{E_{12}(E_{12}+E_G)\frac{\alpha^2}{R}\frac{b}{\pi} - E_2(E_1\alpha^2+E_G)\frac{b}{\pi R}}{(E_1\alpha^2+E_G)(E_2+E_G\alpha^2)-(E_{12}+E_G)^2\alpha^2}. \tag{3.4}$$

An iterative procedure is used to determine the numerically smallest critical stress σ_c, the corresponding value(s) of the axial waveparameter α and the instantaneous moduli, for given material and given values of h, b and R.

In the elastic range it is well known that bifurcation of a complete unstiffened shell occurs at $\sigma_c = -\{3(1-\nu^2)\}^{-1/2}Eh/R$, with several simultaneous buckling modes [2]. These include the axisymmetric modes and the modes with circumferential wave number m up to a certain limiting value, above which the bifurcation stress increases with increasing m. Figure 2 illustrates this for a rather thick shell, where the limiting value of m is between 12 and 13. In the plastic range the modulus E_1 decreases more rapidly than the other prebuckling moduli. Therefore, the plastic bifurcation stress is smallest for the axisymmetric mode and increases with increasing circumferential wave number. An example of this is also shown in Fig. 2, for $\sigma_y/E = 0.002$.

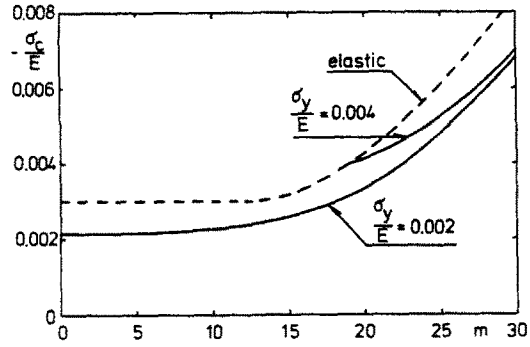

Fig. 2. Bifurcation stress versus circumferential wave number for complete unstiffened cylindrical shell with $R/h = 200$, $n = 10$, $\nu = 0.3$.

In a stiffened shell with stringers located at $x^2 = b/2 \pm kb$ (for integer k) the bifurcation modes (3.1) are still valid, provided that the only constraint along the stiffeners is the suppression of radial deflection waves. Thus, the bifurcation stress for the cylindrical panel is also given by the expression (3.2). Koiter[1] has found that for a sufficiently narrow cylindrical panel in the elastic range the bifurcation stress (3.2) reduces to

$$\sigma_c = -E\frac{\pi^2 h^2}{3(1-\nu^2)b^2}(1+\theta^4), \qquad \theta = \frac{\sqrt[4]{[12(1-\nu^2)]}}{2\pi}\frac{b}{\sqrt{(Rh)}}. \tag{3.5}$$

This elastic bifurcation stress is valid for $\theta \leq 1$, with only one critical wave parameter $\alpha = 1$. For $\theta > 1$ the earlier mentioned critical stress for the complete elastic shell is valid, with two critical α-values for each circumferential wave number m.

For a cylindrical panel that bifurcates in the plastic range we shall also use the parameter θ to characterize the "flatness" of the panel. Here again we find two critical α-values for each value of θ in the range $\theta > 1$, and also in certain ranges of θ values below unity, dependent on the values of σ_c/σ_y and n. In the present investigation the main interest is devoted to cases where only a single bifurcation mode (one α-value) is associated with the critical stress. Examples of such cases are shown later in Figs. 3 and 4.

An asymptotic theory of initial post-bifurcation behaviour in the plastic range has been developed by Hutchinson[6, 7], which extends Hill's general theory of bifurcation in elastic-plastic solids[11, 12]. As in Koiter's elastic post-buckling theory[2] the load in the vicinity of the bifurcation point is expanded in terms of the buckling mode amplitude, but in the plastic range the analysis is further complicated by the necessity to account for elastic unloading.

In a case where the buckling mode is unique, the asymptotically exact expression for the load parameter λ in terms of the buckling mode amplitude ξ is obtained of the form

$$\lambda = \lambda_c + \lambda_1\xi + \lambda_2\xi^{1+\beta} + \cdots \tag{3.6}$$

for $\xi \geq 0$. Here, we normalize the buckling mode so that for $\xi = 1$ the maximum normal deflection w is equal to the shell thickness. The constant λ_1 is determined by the requirement that plastic loading takes place throughout the current plastic zone, except in at least one point where neutral loading takes place. After bifurcation a region of elastic unloading spreads into the material from each of these neutral loading points, and the effect of these unloading regions is accounted for to lowest order in the third term of the expansion (3.6).

For the cylindrical panels considered elastic unloading starts on the outside of the shell at the points of maximum outward deflection. In the limiting case of a flat plate ($\theta = 0$) unloading starts simultaneously at the points of maximum outward- and inward deflection. The value of the parameter β depends on the shape of the unloading regions spreading into the material[7], and here we find $\beta = 1/3$. The constant λ_2 is found negative in all cases, so that the truncated expansion (3.6) can be used to estimate the maximum support load, which is slightly above the critical bifurcation load. The values of the constants σ_c, λ_1 and λ_2 are given in Table 1 for a few

Table 1. Constants in asymptotic post-bifurcation expansion for various cylindrical panels

h/b	θ	σ_y/E	ν	n	$-\sigma_c/\sigma_y$	λ_1/λ_c	λ_2/λ_c	β
0.025	0.50	0.0020	0.3	10	1.104	0.643	−1.91	1/3
0.025	0.50	0.0020	0.3	3	1.162	0.884	−3.59	1/3
0.025	0.75	0.0028	0.3	10	1.033	0.804	−3.49	1/3
0.025	0.75	0.0028	0.3	3	1.052	0.878	−4.84	1/3

examples of cylindrical panels that bifurcate in the plastic range with only a single bifurcation mode.

It is known that bifurcation stresses obtained by J_2-deformation theory are often in better agreement with experiments than the predictions of J_2-flow theory[7]. However, for the cases considered in Table 1 bifurcation does not occur far into the plastic range, so the discrepancy is rather small with a maximum of 1.7% corresponding to the case $\theta = 0.5$, $n = 10$.

4. ASYMPTOTIC ANALYSIS WITH NO ELASTIC UNLOADING

The effect of a small initial imperfection on a structure compressed into the plastic range has not yet been described by a simple asymptotic formula such as those obtained by Koiter[2] for the elastic range. The main difficulty, is that an asymptotic expansion of the initial part of the equilibrium solution is only valid up to the point at which elastic unloading starts, while a second expansion that accounts for the growing elastic unloading region is required to represent the remaining part of the equilibrium path[13]. Also, the maximum support load of a perfect elastic–plastic structure is attained at a limit point after finite buckling mode deflections and not at the bifurcation point as in the elastic range.

Here, we shall analyse the imperfection-sensitivity on the basis of J_2-flow theory, but with elastic unloading neglected. By using this hypoelastic theory the difficulties mentioned above are avoided and an asymptotic estimate is obtained for the imperfection-sensitivity of the hypoelastic cylindrical panel. This approach has been used earlier by Hutchinson and Budiansky[8] for the case of a cruciform column, and by Needleman and Tvergaard[9] for the case of an axially compressed square plate. The cruciform has the special property that, often, no strain rate reversal occurs before the maximum load, so that neglecting elastic unloading is completely justified. For the plate strain rate reversal does occur slightly before the maximum load. However, the results of Ref. [9] show that the hypoelastic expansion gives a reasonable estimate of the imperfection-sensitivity of an elastic–plastic plate. Here, the asymptotic expansion based on hypoelastic theory shall be extended to cover shell behaviour, and shall be used for the cylindrical panel. As the expansion has been described in detail for the plate[9], only the main steps are given here.

The perfect shell made of hypoelastic material has the same bifurcation stress as the corresponding elastic–plastic shell, but instead of (3.6) the initial post-bifurcation expansion in the case of a unique buckling mode takes the form

$$\lambda = \lambda_c + \lambda_1{}^{he}\xi + \lambda_2{}^{he}\xi^2 + \cdots \tag{4.1}$$

$$\left.\begin{aligned} v_\alpha &= v_\alpha{}^0 + \overset{(1)}{v}_\alpha\xi + \overset{(2)}{v}_\alpha\xi^2 + \cdots \\ w &= w^0 + \overset{(1)}{w}\xi + \overset{(2)}{w}\xi^2 + \cdots \end{aligned}\right\} \tag{4.2}$$

where the higher order contributions are taken to be orthogonal to the bifurcation mode

$$\int_A N_c{}^{\alpha\beta}\overset{(1)}{w}_{,\alpha}\overset{(i)}{w}_{,\beta}\,\mathrm{d}A = 0, \quad \text{for } i > 1. \tag{4.3}$$

The plastic branches of the J_2-flow theory moduli are functions only of the stresses, and can be expanded in a Taylor series about the bifurcation point

$$\hat{L}^{\alpha\beta\gamma\delta} = \hat{L}_c^{\alpha\beta\gamma\delta} + \left.\frac{\partial \hat{L}^{\alpha\beta\gamma\delta}}{\partial \sigma^{\mu\nu}}\right|_c (\sigma^{\mu\nu} - \sigma_c^{\mu\nu}) + \frac{1}{2}\left.\frac{\partial^2 \hat{L}^{\alpha\beta\gamma\delta}}{\partial \sigma^{\mu\nu}\partial \sigma^{\rho\omega}}\right|_c (\sigma^{\mu\nu} - \sigma_c^{\mu\nu})(\sigma^{\rho\omega} - \sigma_c^{\rho\omega}) + \cdots \tag{4.4}$$

Substituting (4.2) into (2.1) gives the expansion of the strains, and the similar expansion of the stresses is related to the strains by using (2.7) and (4.4).

Expressions for the parameters λ_1^{he}, λ_2^{he} etc. are obtained by substituting the expansions into the incremental principle of virtual work (2.11). Hutchinson[7] has given the expression for λ_1^{he}, which is zero for the cylindrical panel due to symmetry. The expression for λ_2^{he} is considerably simplified if $\lambda_1^{he} = 0$, in which case we find

$$\lambda_2^{he} = -\frac{\mathscr{C}}{D} \tag{4.5}$$

$$\begin{aligned}\mathscr{C} = &\int_A \{3\overset{(2)}{N}{}^{\alpha\beta}\overset{(1)}{w}_{,\alpha}\overset{(1)}{w}_{,\beta} + 6\overset{(1)}{N}{}^{\alpha\beta}\overset{(1)}{w}_{,\alpha}\overset{(2)}{w}_{,\beta}\}\,dA \\ &+ \int_V \left\{\overset{(2)}{\sigma}{}^{\mu\nu}\left.\frac{\partial \hat{L}^{\alpha\beta\gamma\delta}}{\partial \sigma^{\mu\nu}}\right|_c \overset{(1)}{\eta}_{\alpha\beta}\overset{(1)}{\eta}_{\gamma\delta} + 2\overset{(1)}{\sigma}{}^{\mu\nu}\left.\frac{\partial \hat{L}^{\alpha\beta\gamma\delta}}{\partial \sigma^{\mu\nu}}\right|_c \overset{(1)}{\eta}_{\alpha\beta}\overset{(2)}{\eta}_{\gamma\delta}\right. \\ &\left. + \frac{1}{2}\overset{(1)}{\sigma}{}^{\mu\nu}\overset{(1)}{\sigma}{}^{\rho\omega}\left.\frac{\partial^2 \hat{L}^{\alpha\beta\gamma\delta}}{\partial \sigma^{\mu\nu}\partial \sigma^{\rho\omega}}\right|_c \overset{(1)}{\eta}_{\alpha\beta}\overset{(1)}{\eta}_{\gamma\delta}\right\} dV\end{aligned} \tag{4.6}$$

$$\begin{aligned}D = &\int_A \left\{6\overset{(1)}{N}{}^{\alpha\beta}\frac{\partial w_\alpha^0}{\partial \lambda}\right|_c \overset{(1)}{w}_{,\beta} + 3\frac{\partial N_0^{\alpha\beta}}{\partial \lambda}\Big|_c \overset{(1)}{w}_{,\alpha}\overset{(1)}{w}_{,\beta}\Big\}\,dA \\ &+ \int_V \left\{\left.\frac{\partial \sigma_0^{\mu\nu}}{\partial \lambda}\right|_c \left.\frac{\partial \hat{L}^{\alpha\beta\gamma\delta}}{\partial \sigma^{\mu\nu}}\right|_c \overset{(1)}{\eta}_{\alpha\beta}\overset{(1)}{\eta}_{\gamma\delta} + 2\overset{(1)}{\sigma}{}^{\mu\nu}\left.\frac{\partial \hat{L}^{\alpha\beta\gamma\delta}}{\partial \sigma^{\mu\nu}}\right|_c \left.\frac{\partial \eta_{\alpha\beta}^0}{\partial \lambda}\right|_c \overset{(1)}{\eta}_{\gamma\delta}\right\} dV\end{aligned} \tag{4.7}$$

where V is the volume of shell material corresponding to the middle surface area A.

The expressions (4.6) and (4.7) depend on the second order contributions to the asymptotic expansions, which are found by solution of a variational equation obtained from the principle of virtual work. For $\lambda_1^{he} = 0$ the variational equation takes the form

$$\int_A \{\overset{(2)}{M}{}^{\alpha\beta}\delta\kappa_{\alpha\beta} + \overset{(2)}{N}{}^{\alpha\beta}\delta^c\epsilon_{\alpha\beta} + N_c^{\alpha\beta}\overset{(2)}{w}_{,\alpha}\delta w_{,\beta} + \overset{(1)}{N}{}^{\alpha\beta}\overset{(1)}{w}_{,\alpha}\delta w_{,\beta}\}\,dA = 0 \tag{4.8}$$

$$\overset{(2)}{\sigma}{}^{\alpha\beta} = \hat{L}_c^{\alpha\beta\gamma\delta}\overset{(2)}{\eta}_{\gamma\delta} + \frac{1}{2}\overset{(1)}{\sigma}{}^{\mu\nu}\left.\frac{\partial \hat{L}^{\alpha\beta\gamma\delta}}{\partial \sigma^{\mu\nu}}\right|_c \overset{(1)}{\eta}_{\gamma\delta} \tag{4.9}$$

$$\overset{(2)}{\eta}_{\gamma\delta} = \frac{1}{2}(\overset{(2)}{v}_{\gamma,\delta} + \overset{(2)}{v}_{\delta,\gamma}) - d_{\gamma\delta}\overset{(2)}{w} + \frac{1}{2}\overset{(1)}{w}_{,\gamma}\overset{(1)}{w}_{,\delta} - x^3\overset{(2)}{w}_{,\gamma\delta} \tag{4.10}$$

where $\overset{(2)}{N}{}^{\alpha\beta}$ and $\overset{(2)}{M}{}^{\alpha\beta}$ are obtained from (2.10) using (4.9) and (4.10). The solutions $\overset{(2)}{v}_1$, $\overset{(2)}{v}_2$, $\overset{(2)}{w}$ are periodic in axial direction, and are the same in all panels, as they grow proportionally with ξ^2 while neighbouring panels have identical bifurcation modes with opposite signs of the amplitudes. Thus, the second order mode displacements are symmetric about the line of attachment of a stiffener, in addition to the symmetry about the panel centre lines.

The load terms in eqn (4.8) suggest that the boundary value problem has a solution of the form

$$\left.\begin{aligned}\overset{(2)}{v}_1 &= \bar{\epsilon}x^1 + \bar{v}_1 \sin\frac{2\alpha\pi x^1}{b} \\ \overset{(2)}{v}_2 &= \bar{v}_2 + \tilde{v}_2 \cos\frac{2\alpha\pi x^1}{b} \\ \overset{(2)}{w} &= \bar{w} + \tilde{w} \cos\frac{2\alpha\pi x^1}{b}\end{aligned}\right\} \tag{4.11}$$

where $\bar{\epsilon}$ is a constant, and $\bar{v}_2$, $\bar{w}$, $\tilde{v}_1$, $\tilde{v}_2$ and $\tilde{w}$ are functions of x^2. Furthermore, this solution satisfies the orthogonality condition (4.3). With the solution (4.11) the variational equation separates into two independent boundary value problems in the interval $0 \le x^2 \le b/2$, one for the $\bar{(\ )}$-quantities and one for the $\tilde{(\ )}$-quantities. Each of these problems is solved numerically by making a finite element approximation of the x^2-dependent functions in terms of Hermitian cubics. The $\bar{(\ )}$-quantities automatically satisfy the constraint (2.13) and thus have the boundary conditions (2.12) at both ends of the interval $x^2 = 0$, $b/2$. For the $\tilde{(\ )}$-quantities the boundary conditions are (2.12) at $x^2 = 0$, and at $x^2 = b/2$ the boundary conditions are the three first conditions in (2.12) and the condition $\tilde{w} = 0$, which results from (2.13). Furthermore, according to (2.14) the integral of $\overset{(2)}{N}{}^{11}$ over the panel width must vanish.

The imperfections considered in this analysis are taken in the shape of the critical bifurcation mode (3.1) with amplitude $\bar{\xi}$. The asymptotic analysis of the influence of such imperfections is divided into a singular perturbation analysis valid for λ near λ_c, a regular perturbation analysis valid for $\lambda < \lambda_c$, and finally the matching of these two results [8, 9].

The singular perturbation analysis gives the following asymptotic expression for λ as a function of ξ, in the vicinity of λ_c,

$$\lambda = \lambda_c + \lambda_2^{hc}\xi^2 + c\bar{\xi}^k\xi^{-1/\psi} + \cdots \tag{4.12}$$

where the constants c and k are undetermined by the analysis, and

$$\psi = 1 + \frac{\beta_1}{\beta_2} \tag{4.13}$$

$$\beta_1 = \int_A \left\{ \frac{\partial \hat{L}^{\alpha\beta\gamma\delta}}{\partial \sigma^{\mu\nu}}\bigg|_c \overset{(1)}{\kappa}_{\alpha\beta} \left(\overset{(1)}{M}{}^{\mu\nu} \frac{\partial e^0_{\gamma\delta}}{\partial \lambda}\bigg|_c - \frac{h^3}{12}\frac{\partial \sigma_0{}^{\mu\nu}}{\partial \lambda}\bigg|_c \overset{(1)}{\kappa}_{\gamma\delta} \right) + \frac{\partial \hat{L}^{\alpha\beta\gamma\delta}}{\partial \sigma^{\mu\nu}}\bigg|_c \overset{(1)}{e}_{\alpha\beta} \left(\overset{(1)}{N}{}^{\mu\nu} \frac{\partial e^0_{\gamma\delta}}{\partial \lambda}\bigg|_c - h\frac{\partial \sigma_0{}^{\mu\nu}}{\partial \lambda}\bigg|_c \overset{(1)}{e}_{\gamma\delta} \right) \right\} dA \tag{4.14}$$

$$\beta_2 = \int_A \left\{ \frac{\partial \hat{L}^{\alpha\beta\gamma\delta}}{\partial \sigma^{\mu\nu}}\bigg|_c \frac{\partial \sigma_0{}^{\mu\nu}}{\partial \lambda}\bigg|_c \left(\frac{h^3}{12} \overset{(1)}{\kappa}_{\alpha\beta} \overset{(1)}{\kappa}_{\gamma\delta} + h \overset{(1)}{e}_{\alpha\beta} \overset{(1)}{e}_{\gamma\delta} \right) + \frac{\partial N_0{}^{\alpha\beta}}{\partial \lambda}\bigg|_c \overset{(1)}{w}_{,\alpha} \overset{(1)}{w}_{,\beta} \right\} dA. \tag{4.15}$$

Here, and in the following $e_{\alpha\beta}$ denotes the linear part of the membrane strain tensor $\epsilon_{\alpha\beta}$. For an elastic material, linear or nonlinear, the parameter ψ equals unity.

In the regular perturbation analysis the lowest order effect of a small imperfection is determined for $\lambda < \lambda_c$. The displacements, strains and stresses are written as

$$v_\alpha = v_\alpha{}^0 + \tilde{v}_\alpha, \quad w = w^0 + \tilde{w}, \quad \eta_{\alpha\beta} = e^0_{\alpha\beta} + \tilde{\eta}_{\alpha\beta}, \quad \sigma^{\alpha\beta} = \sigma_0{}^{\alpha\beta} + \tilde{\sigma}^{\alpha\beta} \tag{4.16}$$

where the solution for the perfect shell at the current load level λ is denoted by $(\ )^0$, while $\tilde{(\ )}$ denotes small perturbation quantities that vanish at $\lambda = 0$. All equations are linearized with respect to the small perturbation- and imperfection quantities. Thus, the constitutive equation (2.7) yields the linearized relation

$$\frac{d\tilde{\sigma}^{\alpha\beta}}{d\lambda} = \hat{L}_0{}^{\alpha\beta\gamma\delta} \frac{d\tilde{\eta}_{\gamma\delta}}{d\lambda} + \frac{\partial \hat{L}^{\alpha\beta\gamma\delta}}{\partial \sigma^{\mu\nu}}\bigg|_0 \tilde{\sigma}^{\mu\nu} \frac{de^0_{\gamma\delta}}{d\lambda} \tag{4.17}$$

and the linearized principle of virtual work takes the form

$$\int_A \{\tilde{N}^{\alpha\beta}\delta e_{\alpha\beta} + \tilde{M}^{\alpha\beta}\delta\kappa_{\alpha\beta} + N_0{}^{\alpha\beta}(\tilde{w}_{,\alpha} + \bar{\xi}\overset{(1)}{w}_{,\alpha})\delta w_{,\beta}\}\, dA = 0. \tag{4.18}$$

To solve eqn (4.18), we expand $\tilde{v}_\alpha$ and $\tilde{w}$ in terms of the set of eigenfunctions of the form (3.1), with any integer number of halfwaves along the length of the shell and over the width of the panel. We also use the fact that both $\hat{L}_0{}^{\alpha\beta\gamma\delta}$ and

$$\frac{\partial \hat{L}^{\alpha\beta\gamma\delta}}{\partial \sigma^{\mu\nu}}\bigg|_0 \frac{\mathrm{d}e^0_{\gamma\delta}}{\mathrm{d}\lambda}$$

appearing in (4.17) are orthotropic fourth order tensors in the sense

$$C^{\alpha\beta\gamma\delta} = C^{\beta\alpha\gamma\delta} = C^{\alpha\beta\delta\gamma}, \quad C^{1211} = C^{1222} = C^{1112} = C^{2212} = 0. \tag{4.19}$$

This property is employed together with the fact that for each eigenfunction in the expansion also the corresponding $e_{\alpha\beta}$ and $\kappa_{\alpha\beta}$ vary as sines or cosines, and the result is a complete decoupling of the equations for the eigenmode amplitudes. Finally we find that the variation of the amplitude ξ of the critical eigenmode (3.1) can be written on the form [9]

$$\xi = \bar{\xi}\left(1 - \frac{\lambda}{\lambda_c}\right)^{-\psi} p(\lambda) \tag{4.20}$$

where ψ is given by (4.13) and $p(\lambda)$ is finite at $\lambda = \lambda_c$. The function $p(\lambda)$, and in particular the value $p(\lambda_c)$, is computed by using the eigenmode expansion in (4.18) and (4.17) and solving for increasing λ in the interval $0 \le \lambda < \lambda_c$ (see Appendix).

Matching of the expression (4.20) with the rising part of (4.12) in the vicinity of $\lambda = \lambda_c$ determines the values of the two constants c and k

$$c = -\lambda_c [p(\lambda_c)]^{1/\psi}, \qquad k = 1/\psi. \tag{4.21}$$

Now, according to the expression (4.12), with the values (4.21) substituted, the hypoelastic structure is imperfection-sensitive provided that $\lambda_2^{he} < 0$. In that case an imperfection of amplitude $\bar{\xi}$ converts the bifurcation buckling into snap buckling at a reduced load λ_s given by the asymptotic estimate

$$\frac{\lambda_s}{\lambda_c} = 1 - \mu \bar{\xi}^{2/(2\psi+1)} \tag{4.22}$$

$$\mu = \left[-\frac{\lambda_2^{he}}{\lambda_c}\right]^{1/(2\psi+1)} (2\psi+1)(2\psi)^{-2\psi/(2\psi+1)} [p(\lambda_c)]^{2/(2\psi+1)}. \tag{4.23}$$

Numerically obtained values of the bifurcation stress σ_c and of the hypoelastic post-bifurcation coefficient λ_2^{he} are given in Figs. 3 and 4 as functions of the flatness parameter θ. The panels considered have a fixed thickness to width ratio $h/b = 0.025$, but various levels of yield stress are considered, with strain hardening exponent $n = 10$ in Fig. 3 and $n = 3$ in Fig. 4. The curves are only drawn in the ranges, where a single axial wave parameter α is associated with σ_c. Clearly, the change from one to two critical α-values occurs closer to the yield stress when θ is closer to unity.

For the elastic panel λ_2^{he}/λ_c reduces exactly to the corresponding elastic post-bifurcation coefficient, with the value $\frac{3}{8}(1-\nu^2)$ in the plate case ($\theta = 0$), and with the change from stable- to unstable post-bifurcation behaviour at $\theta \approx 0.64$, as obtained by Koiter [1]. For low strain hardening, Fig. 3, the material nonlinearities result in imperfection-sensitivity, even at small θ-values. At the larger θ-values material nonlinearities and geometric non-linearities contribute about equally to the imperfection-sensitivity, so that λ_2^{he} is close to the corresponding elastic value. For the high hardening material, Fig. 4, a stable post-bifurcation behaviour is found for small θ-values, but the change to unstable behaviour occurs at a smaller value of θ than that found for the elastic panel. Both in Fig. 3 and Fig. 4 we note that the values of λ_2^{he}, as functions of θ, are discontinuous at the points where σ_c equals the yield stress, because the moduli-derivatives are discontinuous at the yield stress.

Some values obtained for λ_2^{he}, ψ, $p(\lambda_c)$ and μ are given in Table 2. For comparison, the value of $p(\lambda_c)$ obtained in the elastic range (with linear prebuckling) is unity, so that with $\psi = 1$ the expression (4.23) for μ reduces to the well-known result for elastic buckling. It is of interest to note that the values of μ obtained in Table 2 are smaller (down to 25%) than those obtained

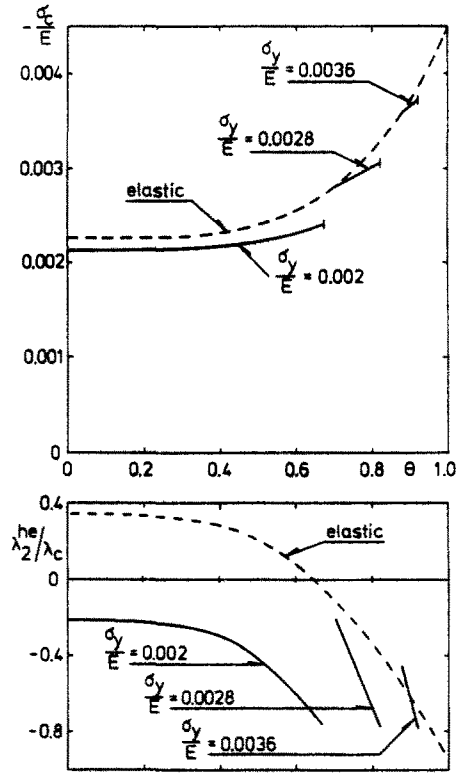

Fig. 3.

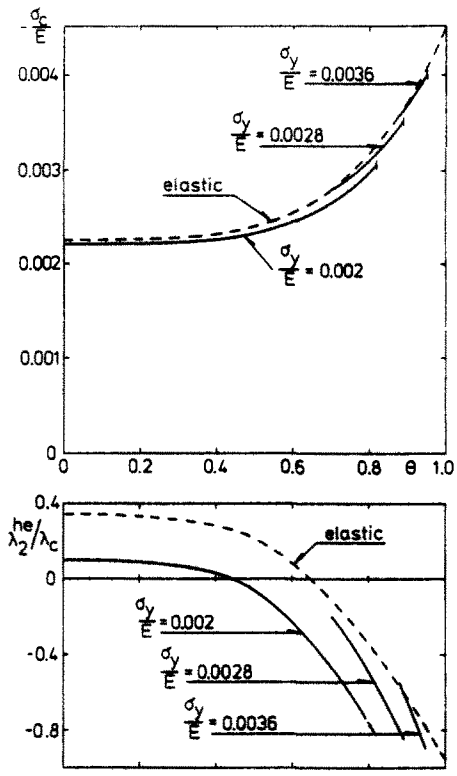

Fig. 4.

Fig. 3. Bifurcation stress and hypoelastic post-bifurcation coefficient versus flatness parameter for elastic-plastic cylindrical panels with $h/b = 0.025$, $n = 10$, $\nu = 0.3$. The curves are only drawn in the range, where the wave parameter α is unique.

Fig. 4. Bifurcation stress and hypoelastic post-bifurcation coefficient versus flatness parameter for elastic-plastic cylindrical panels with $h/b = 0.025$, $n = 3$, $\nu = 0.3$. The curves are only drawn in the range, where the wave parameter α is unique.

Table 2. Constants in hypoelastic asymptotic analysis for cylindrical panels with $h/b = 0.025$ and $\nu = 0.3$

θ	σ_y/E	n	$-\sigma_c/\sigma_y$	λ_2^{he}/λ_c	ψ	$p(\lambda_c)$	μ
0.50	0.0020	10	1.104	−0.414	1.716	0.045	0.344
0.50	0.0020	3	1.162	−0.059	1.231	0.421	0.489
0.75	0.0028	10	1.033	−0.430	1.150	0.278	0.658
0.75	0.0028	3	1.052	−0.330	1.071	0.628	0.978

by the elastic formula, for the same values of λ_2^{he}/λ_c. In the next section the values given in Table 2 shall be used to compare the asymptotic estimate of imperfection-sensitivity with numerical results.

5. NUMERICAL COMPUTATION OF IMPERFECTION-SENSITIVITY

The behaviour of imperfect panels is here computed numerically by an incremental procedure based on the variational equation (2.11). As in the preceding section, the imperfections considered are taken in the shape of the critical bifurcation mode (3.1) with amplitude $\bar{\xi}$.

In the numerical method employed to solve (2.11) the displacements are expanded in terms of trigonometric functions in the axial direction, while a one-dimensional finite element approximation is used in the circumferential direction.

$$\begin{Bmatrix} v_1 \\ v_2 \\ w \end{Bmatrix} = \begin{Bmatrix} U^{(0)}(x^2)\alpha\dfrac{x^1}{b} \\ V^{(0)}(x^2) \\ W^{(0)}(x^2) \end{Bmatrix} + \sum_{n=1}^{N} \begin{Bmatrix} U^{(n)}(x^2)\cos\dfrac{n\alpha\pi x^1}{b} \\ V^{(n)}(x^2)\sin\dfrac{n\alpha\pi x^1}{b} \\ W^{(n)}(x^2)\sin\dfrac{n\alpha\pi x^1}{b} \end{Bmatrix}. \tag{5.1}$$

Here, the functions $U^{(i)}(x^2)$, $V^{(i)}(x^2)$ and $W^{(i)}(x^2)$ are approximated by Hermitian cubics within each finite element, and the wave parameter α is that corresponding to the critical bifurcation stress. This method has also been used for an axially compressed oval cylindrical shell[14], within the context of a more accurate shell theory.

The boundary conditions specified are the symmetry conditions (2.12) at the panel centres in addition to the stiffener constraint (2.13), which gives $W^{(i)}(b/2) = 0$ for $i \geq 1$. In the expansion (5.1) it is found that $N = 2$ gives good accuracy, with a half panel width divided into 2 elements. The integrals in eqn (2.11) are evaluated by 4 point Gaussian quadrature in circumferential direction within each element, while in the axial direction it is found sufficient to divide the interval $-\frac{1}{2}b/\alpha \leq x^1 \leq \frac{1}{2}b/\alpha$ in two subintervals, using 4 point Gaussian quadrature within each subinterval. Through the thickness Simpson's rule is used, with 7 points in (2.10).

The active branch of the tensor of moduli (2.8) at an integration point is determined in each increment as follows. If the stress state at the integration point is on its current yield surface, the plastic branch is taken to be active. If $\dot{\sigma}_e$ for that integration point turns out to be negative, the elastic branch is taken to be active in the next loading increment. This procedure is sufficiently accurate if small increments are used and if the transition from loading to unloading, or vice versa, occurs only once or twice during the loading history.

The results of numerical computations shown in Figs. 5–8 give the load parameter λ as a function of the deflection contribution $W_1 = W^{(1)}(0)$, which is quite a good measure of the bifurcation mode growth. All the results are computed for $h/b = 0.025$ and $\nu = 0.3$, with strain hardening exponent $n = 10$ in the first two figures and $n = 3$ in the last two figures. The flatness parameter and the yield stress are taken as $\theta = 0.5$ and $\sigma_y/E = 0.002$ in Figs. 5 and 7, while the values used in Figs. 6 and 8 are $\theta = 0.75$ and $\sigma_y/E = 0.0028$.

The post-bifurcation behaviour of the perfect panel is computed numerically as the behaviour of a panel with a small initial imperfection $\bar{\xi} = 0.0002$. In all four figures this behaviour

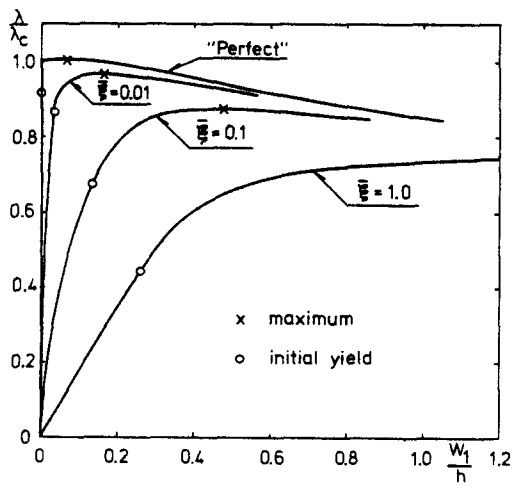

Fig. 5.

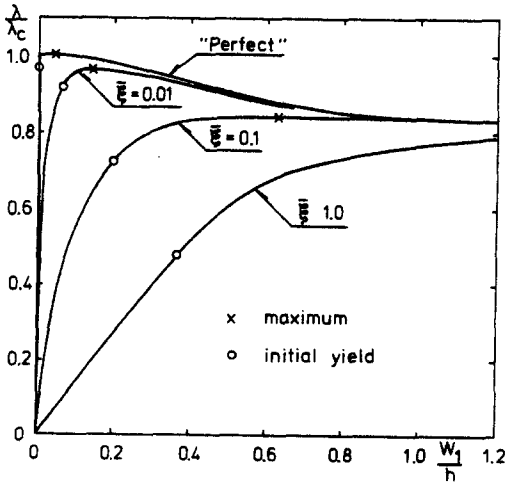

Fig. 6.

Fig. 5. Load versus mode deflection for cylindrical panel that bifurcates in the plastic range ($h/b = 0.025$, $\theta = 0.5$, $\sigma_y/E = 0.002$, $n = 10$, $\nu = 0.3$).

Fig. 6. Load versus mode deflection for cylindrical panel that bifurcates in the plastic range ($h/b = 0.025$, $\theta = 0.75$, $\sigma_y/E = 0.0028$, $n = 10$, $\nu = 0.3$).

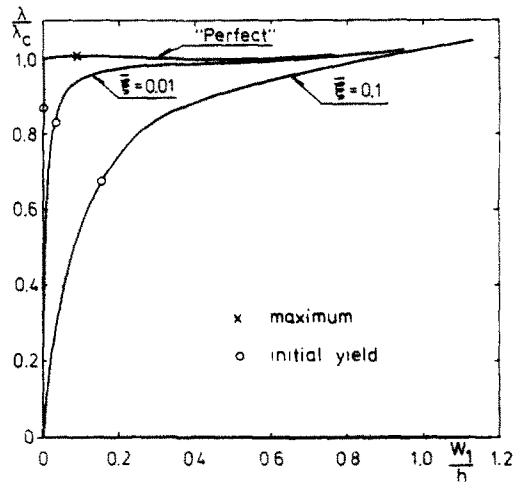

Fig. 7.

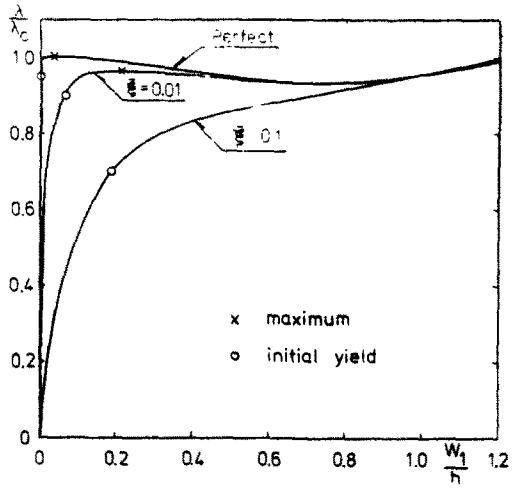

Fig. 8.

Fig. 7. Load versus mode deflection for cylindrical panel that bifurcates in the plastic range ($h/b = 0.025$, $\theta = 0.5$, $\sigma_y/E = 0.002$, $n = 3$, $\nu = 0.3$).

Fig. 8. Load versus mode deflection for cylindrical panel that bifurcates in the plastic range ($h/b = 0.025$, $\theta = 0.75$, $\sigma_y/E = 0.0028$, $n = 3$, $\nu = 0.3$).

is seen to agree with the asymptotic expansion (3.6) in that bifurcation takes place under increasing load and in that a maximum is reached slightly above the bifurcation load after a finite bifurcation mode deflection. As this characteristic behaviour results from the effect of elastic unloading, it is not predicted by the hypoelastic post-bifurcation expansion (4.1). However, the hypoelastic expansion with the values obtained for λ_2^{he}/λ_c (Table 2) does agree well with the general trend of the numerically computed post-bifurcation behaviour in each of Figs. 5–8, apart from the maximum just after bifurcation.

The shell considered in Fig. 5 is in the range of θ-values, where elastic cylindrical panels have a stable post-buckling behaviour. The elastic–plastic panel with $n = 10$ is clearly imperfection sensitive. For the largest imperfection considered, $\bar{\xi} = 1.0$, a maximum is not reached in the range considered, but the curve flattens out at a level of reduced support load.

In Fig. 6, for a more curved panel with a higher yield stress, but still with the strain hardening exponent $n = 10$, the behaviour is quite similar to that obtained in Fig. 5. The sensitivity to small imperfections is slightly higher, but for the largest imperfection the support load is a little less reduced.

The cylindrical panel considered in Fig. 7 is identical to that of Fig. 5, except that the material is high hardening with $n = 3$. For the perfect panel the post-bifurcation load after the maximum decreases to a value slightly below the bifurcation load, in agreement with the small negative value obtained for λ_2^{he}/λ_c, but then starts to increase again in the more advanced post-buckling range. The result is that even for the small imperfection, $\bar{\xi} = 0.01$, no maximum is found before the support load exceeds the bifurcation load.

The panel in Fig. 8 is that of Fig. 6, with the strain hardening exponent changed to $n = 3$. The behaviour is much like that found in Fig. 7, but the post-bifurcation load reaches a considerably lower level before again starting to increase in the advanced post-buckling range. In this case a local maximum is found for $\bar{\xi} = 0.01$, but not for $\bar{\xi} = 0.1$.

A comparison between the numerical results and the asymptotic estimate (4.22) of the imperfection-sensitivity is given in Fig. 9. Here the curve (4.22) is drawn on the basis of the parameters ψ and μ given in Table 2, and the numerically computed support loads are indicated by a dot for $\bar{\xi} = 0.0002$, $\bar{\xi} = 0.01$ and $\bar{\xi} = 0.1$. In Figs. 9(a) and (b), corresponding to Figs. 5 and 6, the agreement is very good for the range considered. However, for the large imperfection $\bar{\xi} = 1.0$ the support load is underestimated by the asymptotic analysis, as one would expect.

In Fig. 9(c) the agreement is also good for the smallest imperfection, but for $\bar{\xi} = 0.1$ no maximum is reached in Fig. 8, so the range of validity of the asymptotic expansion is smaller in this case. Such limited range of validity of the asymptotic results has also been found for elastic

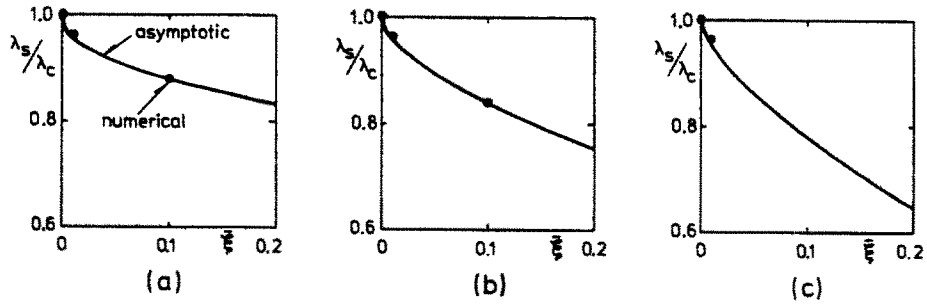

Fig. 9. Comparison of numerical results and asymptotic hypoelastic predictions for the imperfection-sensitivity of elastic-plastic cylindrical panels. (a) Panel with $\theta = 0.5$, $\sigma_y/E = 0.002$, $n = 10$. (b) Panel with $\theta = 0.75$, $\sigma_y/E = 0.0028$, $n = 10$. (c) Panel with $\theta = 0.75$, $\sigma_y/E = 0.0028$, $n = 3$.

buckling behaviour in a number of cases, in which the initially unstable post-buckling behaviour changes to stable behaviour in the advanced post-buckling range[15]. This also agrees with Koiter's conjecture of the advanced post-buckling behaviour for elastic cylindrical panels[1]. The asymptotic results corresponding to Fig. 7 have not been plotted, as no maxima are obtained in this figure for comparison. The value of μ found for this case (Table 2) indicates a great deal of sensitivity to small imperfections, but as the change to stable advanced post-buckling behaviour occurs considerably earlier in Fig. 7 than in Fig. 8 an even smaller range of validity of the asymptotic result must be expected here.

Although the hypoelastic analysis does not account for the effect of elastic unloading, it is found that the asymptotic estimate (4.22) gives a good indication of the imperfection-sensitivity of an elastic–plastic cylindrical panel. This agrees with the results obtained for axially compressed square plates[9]. The range of validity of the asymptotic estimate is found to be smaller for a high hardening material than for a low hardening material, because panels made of a high hardening material have the ability to support loads above the bifurcation load in the advanced post-buckling range. As in Ref. [9] we conclude that the approximation of neglecting elastic unloading in the hypoelastic expansion seems to be less important than the approximation involved in considering lowest order asymptotic results. It may be expected that also for other shell structures the hypoelastic analysis will prove valuable for identifying parameter ranges, where the shells will exhibit imperfection-sensitivity in the plastic range.

REFERENCES

1. W. T. Koiter, Buckling and post-buckling behavior of a cylindrical panel under axial compression. Nationaal *Luchtvaart Laboratorium* **20**, Report S476, Amsterdam (1956).
2. W. T. Koiter, Over de stabiliteit van het elastisch evenwicht. Thesis, Delft, H. J. Paris, Amsterdam (1945) English transl. NASA TT F-10, 833 (1967); and AFFDL-TR-70-25 (1970).
3. W. B. Stephens, Imperfection sensitivity of axially compressed stringer reinforced cylindrical panels under internal pressure. *AIAA J.* **9**, 1713–1719 (1971).
4. G. G. Pope, The buckling behaviour in axial compression of slightly-curved panels, including the effect of shear deformability. *Int. J. Solids Structures* **4**, 323–340 (1968).
5. N. R. Bauld, Imperfection sensitivity of axially compressed stringer reinforced cylindrical sandwich panels. *Int. J. Solids Structures* **10**, 883–902 (1974).
6. J. W. Hutchinson, Post-bifurcation behavior in the plastic range. *J. Mech. Phys. Solids* **21**, 163–190 (1973).
7. J. W. Hutchinson, Plastic buckling. *Advances in Applied Mechanics* (Edited by C. S. Yih), Vol. 14, pp. 67–144. Academic Press, New York (1974).
8. J. W. Hutchinson and B. Budiansky, Analytical and numerical study of the effects of initial imperfections on the inelastic buckling of a cruciform column. *Buckling of Structures* (Edited by B. Budiansky), pp. 98–105. Springer-Verlag, Berlin (1976).
9. A. Needleman and V. Tvergaard, An analysis of the imperfection-sensitivity of square elastic–plastic plates under axial compression. *Int. J. Solids Structures* **12**, 185–201 (1976).
10. V. Tvergaard and A. Needleman, Buckling of eccentrically stiffened elastic–plastic panels on two simple supports or multiply supported. *Int. J. Solids Structures* **11**, 647–663 (1975).
11. R. Hill, A general theory of uniqueness and stability in elastic–plastic solids. *J. Mech. Phys. Solids* **6**, 236–249 (1958).
12. R. Hill, Bifurcation and uniqueness in non-linear mechanics of continua. *Problems of Continuum Mechanics* (S.I.A.M. Philadelphia), 155–164 (1961).
13. J. W. Hutchinson, Imperfection-sensitivity in the plastic range. *J. Mech. Phys. Solids* **21**, 191–204 (1973).
14. V. Tvergaard, Buckling of elastic–plastic oval cylindrical shells under axial compression. *Int. J. Solids Structures* **12**, 683–691 (1976).
15. V. Tvergaard, Buckling behaviour of plate and shell structures. *Proc. 14th Int. Congr. Theor. and Appl. Mech.* (Edited by W. T. Koiter), pp. 233–247. North-Holland, Amsterdam (1976).

APPENDIX

The function $p(\lambda)$ occurring in (4.20), and in particuular the value $p(\lambda_c)$ to be used in (4.21) and (4.23), is determined by integrating the constitutive relation (4.17) and substituting the result into the principle of virtual work.

For the integration of (4.17) it is convenient to write

$$\tilde{\sigma}^{\alpha\beta} = \hat{L}_0^{\alpha\beta\gamma\delta}\tilde{\eta}_{\gamma\delta} + \tilde{Q}^{\alpha\beta}. \tag{A1}$$

Substituted into (4.17) this gives the differential equations for $\tilde{Q}^{\alpha\beta}$

$$\frac{\partial \tilde{Q}^{\alpha\beta}}{\partial\lambda} - R^{\alpha\beta}{}_{\gamma\delta}\tilde{Q}^{\gamma\delta} = S^{\alpha\beta} \tag{A2}$$

where

$$R^{\alpha\beta}{}_{\gamma\delta} = \left.\frac{\partial \hat{L}^{\alpha\beta\mu\nu}}{\partial\sigma^{\gamma\delta}}\right|_0 \frac{\partial e^0_{\mu\nu}}{\partial\lambda} \tag{A3}$$

$$S^{\alpha\beta} = \left[\left.\frac{\partial \hat{L}^{\alpha\beta\mu\nu}}{\partial\sigma^{\mu\nu}}\right|_0 \hat{L}_0^{\mu\nu\gamma\delta} - \left.\frac{\partial \hat{L}^{\alpha\beta\gamma\delta}}{\partial\sigma^{\mu\nu}}\right|_0 \hat{L}_0^{\mu\nu\mu\nu}\right]\frac{\partial e^0_{\mu\nu}}{\partial\lambda}\tilde{\eta}_{\gamma\delta} \tag{A4}$$

In eqn (A2) the differential equation for $\tilde{Q}^{12}$ is uncoupled with the other differential equations, and has the solution

$$\tilde{Q}^{12} = \exp\left[-\int_0^\lambda -2R^{12}{}_{12}\,\mathrm{d}\lambda\right]\int_0^\lambda S^{12}\exp\left[\int_0^\lambda -2R^{12}{}_{12}\,\mathrm{d}\lambda\right]\mathrm{d}\lambda. \tag{A5}$$

The two coupled differential equations for $\tilde{Q}^{11}$ and $\tilde{Q}^{22}$ can be written as uncoupled equations in terms of the two quantities $\tilde{Q}^{11} + r_1\tilde{Q}^{22}$ and $\tilde{Q}^{11} + r_2\tilde{Q}^{22}$, respectively, where

$$\left.\begin{matrix} r_1(\lambda) \\ r_2(\lambda) \end{matrix}\right\} = \frac{R^{22}{}_{22} - R^{11}{}_{11} \pm \sqrt{[(R^{11}{}_{11} - R^{22}{}_{22})^2 + 4R^{22}{}_{11}R^{11}{}_{22}]}}{2R^{22}{}_{11}}. \tag{A6}$$

Explicit solutions of these two equations are obtained of the form

$$\tilde{Q}^{11} + r_1\tilde{Q}^{22} = q_1^{-1}\int_0^\lambda q_1(S^{11} + r_1S^{22})\,\mathrm{d}\lambda \tag{A7}$$

$$\tilde{Q}^{11} + r_2\tilde{Q}^{22} = q_2^{-1}\int_0^\lambda q_2(S^{11} + r_2S^{22})\,\mathrm{d}\lambda \tag{A8}$$

where

$$\begin{aligned} q_1(\lambda) &= \exp\left[\int_0^\lambda -(R^{11}{}_{11} + r_1R^{22}{}_{11})\,\mathrm{d}\lambda\right] \\ q_2(\lambda) &= \exp\left[\int_0^\lambda -(R^{11}{}_{11} + r_2R^{22}{}_{11})\,\mathrm{d}\lambda\right]. \end{aligned} \tag{A9}$$

In the linear elastic range, where the moduli-derivatives vanish, (A6) has no meaning, but here $\tilde{Q}^{\alpha\beta} = 0$ is seen directly.

The expressions obtained for $\tilde{Q}^{\alpha\beta}$ are substituted into (A1), and to satisfy equilibrium these are substituted into the principle of virtual work (4.18), using (2.10). Now, expanding $\tilde{v}_\alpha$ and $\tilde{w}$ and using the orthogonalities due to the orthotropy (4.19), we finally obtain an equation for the bifurcation mode amplitude $\xi(\lambda)$, of the form

$$f_0(\lambda)\xi + \sum_i\left[f_i(\lambda)\int_0^\lambda f_i^*(\lambda)\xi\,\mathrm{d}\lambda\right] + \bar{f}(\lambda)\dot{\xi} = 0 \tag{A10}$$

where f_0, f_i, f_i^* and $\bar{f}$ are known functions of λ. The equation for $p(\lambda)$ is obtained directly by substituting the expression (4.20) into (A10), and the value $p(\lambda_c)$ is obtained by solving successively for increasing λ in the interval $0 \le \lambda < \lambda_c$.